Oxidative Stress Contributes to Lung Injury and Barrier Dysfunction via Microtubule Destabilization

Eric Kratzer[1], Yufeng Tian[1], Nicolene Sarich[1], Tinghuai Wu[1], Angelo Meliton[1], Alan Leff[1], and Anna A. Birukova[1]

[1]Lung Injury Center, Section of Pulmonary and Critical Medicine, Department of Medicine, University of Chicago, Chicago, Illinois

Oxidative stress is an important part of host innate immune response to foreign pathogens, such as bacterial LPS, but excessive activation of redox signaling may lead to pathologic endothelial cell (EC) activation and barrier dysfunction. Microtubules (MTs) play an important role in agonist-induced regulation of vascular endothelial permeability, but their impact in modulation of inflammation and EC barrier has not been yet investigated. This study examined the effects of LPS-induced oxidative stress on MT dynamics and the involvement of MTs in the LPS-induced mechanisms of Rho activation, EC permeability, and lung injury. LPS treatment of pulmonary vascular EC induced elevation of reactive oxygen species (ROS) and caused oxidative stress associated with EC hyperpermeability, cytoskeletal remodeling, and formation of paracellular gaps, as well as activation of Rho, p38 stress kinase, and NF-κB signaling, the hallmarks of endothelial barrier dysfunction. LPS also triggered ROS-dependent disassembly of the MT network, leading to activation of MT-dependent signaling. Stabilization of MTs with epothilone B, or inhibition of MT-associated guanine nucleotide exchange factor (GEF)-H1 activity by silencing RNA-mediated knockdown, suppressed LPS-induced EC barrier dysfunction *in vitro*, and attenuated vascular leak and lung inflammation *in vivo*. LPS disruptive effects were linked to activation of Rho signaling caused by LPS-induced MT disassembly and release of Rho-specific GEF-H1 from MTs. These studies demonstrate, for the first time, the mechanism of ROS-induced Rho activation via destabilization of MTs and GEF-H1–dependent activation of Rho signaling, leading to pulmonary EC barrier dysfunction and exacerbation of LPS-induced inflammation.

Keywords: endothelium; permeability; microtubules; guanine nucleotide exchange factor-H1; LPS

Increased capillary endothelial permeability, along with reduced alveolar liquid clearance capacity, are major pathologic mechanisms of pulmonary edema and its life-threatening complication, the acute respiratory distress syndrome. Mechanisms of endothelial cell (EC) permeability involve dynamic cytoskeletal changes, assembly and disassembly of cell–cell junctions, and signaling crosstalk between various cytoskeletal compartments, such as actin networks and microtubules (MTs) (*see* review in Refs. 1 and 2). It also becomes evident that the cell cytoskeleton plays an important role in the modulation of inflammatory responses. Activation of vascular endothelium by inflammatory mediators increases expression of cell adhesion molecules (intercellular adhesion molecule [ICAM]-1, vascular cell adhesion molecule, E-selectin), which trigger adhesion and tissue transmigration of activated neutrophils (3–5). These events escalate general lung inflammation.

(*Received in original form May 1, 2012 and in final form July 16, 2012*)

This work was supported by the National Heart, Lung, and Blood Institute grants HL089257 and HL107920, and by an American Heart Association Midwest Affiliate Grant-in-Aid.

Correspondence and requests for reprints should be addressed to Anna Birukova, M.D., Lung Injury Center, Section of Pulmonary and Critical Medicine, Department of Medicine, University of Chicago, 5841 S. Maryland Avenue, Office N-613, Chicago, IL 60637. E-mail: abirukov@medicine.bsd.uchicago.edu

Am J Respir Cell Mol Biol Vol 47, Iss. 5, pp 688–697, Nov 2012

Originally Published in Press as DOI: 10.1165/rcmb.2012-0161OC on July 27, 2012
Internet address: www.atsjournals.org

CLINICAL RELEVANCE

In pulmonary endothelium, LPS-induced reactive oxygen species production causes disassembly of microtubule (MT) network and dissociation of Rho-specific guanine nucleotide exchange factor (GEF), GEF-H1, from MTs, which leads to its activation and stimulation of Rho signaling. Activated Rho promotes activation of stress-induced mitogen-activated protein kinases and NF-κB inflammatory cascade, thus leading to endothelial cell barrier dysfunction, increased IL-8 production, intercellular adhesion molecule-1 expression, and IL-8–mediated neutrophil migration. The results of this study suggest that therapeutic strategies directed at mitigation of oxidative stress, stabilization of MTs, and suppression of GEF-H1 activities in the settings of acute lung injury may be a promising direction for future drug design.

Oxidative stress resulting from activation of cellular reactive oxygen species (ROS) production is a part of the innate immune response to foreign pathogens, such as gram-negative bacterial cell wall LPS, and serves as an important mechanism leading to elimination of bacteria. However, uncontrolled activation of ROS production can cause tissue damage, vascular barrier dysfunction, and inflammation. Previous studies identified membrane/cytoplasmic (reduced nicotinamide adenine dinucleotide phosphate oxidase, xanthine oxidoreductase) (6–8) and mitochondrial sources of LPS-activated ROS production (9), and demonstrated redox-sensitive activation of inflammatory signaling, including stress-activated mitogen-activated protein kinases (MAPKs) and NF-κB complex, which further contribute to the mechanisms of inflammation and endothelial barrier dysfunction.

We have demonstrated previously that agonist-induced MT disassembly leads to EC permeability, and release of MT-bound Rho GTPase-specific guanine nucleotide exchange factor (GEF)-H1 triggers a Rho-dependent pathway of actin cytoskeletal remodeling and EC hyperpermeability (10). However, the impact of inflammatory agonist-induced oxidative stress on MT cytoskeletal dynamics, MT-associated signaling, and MT-dependent regulation of EC inflammatory response has not been investigated.

This study tested a hypothesis that LPS-induced oxidative stress may affect MT stability and stimulate alterations in EC permeability and inflammatory signaling via a GEF-H1–dependent mechanism. We used functional, biochemical, imaging, and molecular approaches to characterize LPS-induced changes in MT dynamics, GEF-H1 release, and the resulting activation of inflammatory signaling and barrier dysfunction in pulmonary ECs, and evaluated the role of GEF-H1 in the LPS-induced lung injury *in vivo*.

MATERIALS AND METHODS

Reagents and Cell Culture

Human pulmonary macrovascular ECs (HPAECs) were obtained from Lonza (Allendale, NJ). Antibodies to di-phospho–myosin light

chain (MLC), phospho-p38 MAPK, phospho–heat shock protein (HSP) 27, IκBα, NF-κB, and GEF-H1 were from Cell Signaling (Beverly, MA); phospho–vascular endothelial (VE)-cadherin and ICAM1 were from Santa Cruz Biotechnology (Santa Cruz, CA); phospho-MLC phosphatase was from Millipore (Billerica, MA); phospho-tau antibodies were from Invitrogen (Carlsbad, CA). Epothilone B was purchased from EMD Chemicals (La Jolla, CA). Reagents for immunofluorescence were purchased from Molecular Probes (Eugene, OR). Unless specified, all biochemical reagents were obtained from Sigma (St. Louis, MO).

Measurements of transendothelial electrical resistance (TER) were performed using an electrical cell-substrate impedance sensing system (Applied Biophysics, Troy, NY) (11, 12).

ROS measurement was performed using the Image-iT LIVE Green ROS Detection Kit from Molecular probes (Eugene, OR), according to the manufacturer's recommendations.

MT Fractionation and Western Blot

Isolation of polymerized MTs was performed as previously described (13, 14). Isolation of MT-enriched fraction was performed as described elsewhere (15, 16). Protein extracts were separated by SDS-PAGE, transferred to polyvinylidene difluoride membranes, and incubated with specific antibodies. Equal protein loading was verified by reprobing of membranes with β-tubulin or β-actin antibodies. Immunoreactive proteins were detected using the enhanced chemiluminescent detection system (Amersham, Little Chalfont, UK).

Immunofluorescence Staining and Image Analysis

Immunofluorescence staining of MTs and actin filaments was performed as previously described (11, 12, 17). Slides were analyzed using Nikon video-imaging system (Nikon Instech, Tokyo, Japan). Images were processed using Adobe Photoshop 7.0 software (Adobe Systems, San Jose, CA).

Neutrophil Migration and IL-8 Assays

Neutrophil chemotaxis was measured in a 96-well chemotaxis chamber (Neuroprobe, Gaithersburg, MD), as described previously (18). Concentration of IL-8 was measured using an ELISA kit available from R&D Systems (Minneapolis, MN).

Silencing RNA. Knockdown of GEF-H1 in EC culture and *in vivo* was performed using predesigned standard purity StealthTM GEF-H1–specific silencing (si)RNA sets (Invitrogen, Carlsbad, CA); as previously described (11, 19). Nonspecific, nontargeting RNA (Dharmacon, Lafayette, CO) was used as a control treatment for *in vitro* and *in vivo* experiments.

Animal Studies

All animal care and treatment procedures were approved by the University of Chicago Institutional Animal Care and Use Committee. Animals were handled according to the National Institutes of Health guidelines. Male C57BL/6J mice (Jackson Laboratories, Bar Harbor, ME) were anesthetized and bacterial LPS (0.63 mg/kg; *Escherichia coli* O55:B5, intratracheally) or sterile water was injected with or without epothilone B (4×10^{-6} mol/kg, intravenously) or N-acetyl cysteine (NAC) (2.5×10^{-3} mol/kg, intravenously). In experiments with siRNA, GEF-H1–specific or nonspecific siRNA (2 mg/kg) were intravenously injected 72 hours before LPS administration. After 18 hours, animals were killed under anesthesia. Bronchoalveolar lavage (BAL) was performed as previously described (20, 21).

Statistical Analysis

Results are expressed as means (±SD) of three to eight independent experiments. Stimulated samples were compared by unpaired Student's *t* test. For multiple-group comparisons, one-way ANOVA and *post hoc* multiple comparisons tests were used, and results with *P* values less than 0.05 were considered statistically significant.

RESULTS

Role of Oxidative Stress in LPS-Induced Endothelial Barrier Dysfunction

LPS challenge induced sustained activation of ROS production, with a modest increase observed at 0.5 hour and pronounced ROS production observed after 5 hours of LPS challenge. This result correlated with the time course of LPS-induced permeability increase (Figure 1). Pretreatment with ROS scavenger, NAC, inhibited ROS production in response to LPS (Figure 1A), and significantly attenuated LPS-induced EC hyperpermeability detected by measurements of TER (Figure 1B).

ROS scavenging by NAC prevented LPS-induced actin cytoskeletal remodeling. Immunofluorescence staining of actin cytoskeleton performed after 5 hours of LPS treatment at the time point corresponding to pronounced EC barrier dysfunction showed LPS-induced actin stress fiber formation and disruption of EC monolayer integrity, indicated by paracellular gaps (Figure 1C). These changes were markedly reduced by cell pretreatment with NAC. NAC also attenuated LPS-induced VE-cadherin phosphorylation at Y^{731} (Figure 1D), known to promote disassembly of VE-cadherin containing cell–cell adhesive complexes (22, 23).

Analysis of cell signaling showed that NAC inhibited LPS-induced phosphorylation of myosin-binding subunit of myosin-associated phosphatase type 1 at the Rho kinase–specific site, Y^{850}, and decreased MLC phosphorylation. It also suppressed p38 MAPK cascade, detected by decreased phosphorylation of p38 MAPK and its cytoskeletal target, HSP27, and inhibited NF-κB signaling, as detected by reduced degradation of IκBα-inhibitory subunit (Figure 1E). Collectively, these data emphasize a role of oxidative stress in the development of pulmonary EC barrier failure in response to LPS.

Oxidative Stress Is Involved in LPS-Induced MT Remodeling

MTs play an important role in the regulation of EC permeability (10, 13, 24). The next series of experiments investigated effects of LPS on MT network remodeling. In quiescent endothelium, MT organized into a faint, uniformly distributed lattice network, whereas LPS challenge caused pronounced MT disassembly (Figure 2A). LPS-induced changes in the pool of polymerized MTs were further analyzed using biochemical methods. MT polymerizing agent, epothilone B, and depolymerizing agent, colchicine, were used as positive and negative controls, respectively. Analysis of the MT-enriched fraction (Figure 2B) showed that a majority of tubulin in vehicle-treated cells was present in the polymerized form (assembled MTs). In contrast, LPS-induced MT disassembly detected by cell immunostaining correlated with decreased tubulin content in the MT-enriched fraction and increased depolymerized tubulin content in the cytosolic fraction. Remarkably, NAC pretreatment preserved the MT network against LPS-induced disassembly (Figures 2A and 2B).

The pool of stable MTs undergoes post-translational modifications, such as acetylation and detyrosination (25), which may reflect stability of the MT network under particular conditions (26–28). We analyzed a pool of acetylated and tyrosinated MTs in the LPS-stimulated HPAECs. LPS treatment decreased the pool of acetylated tubulin and increased the pool of tyrosinated tubulin (Figure 2C). Similarly, LPS-induced reduction of acetylated tubulin was also observed in MT-enriched fractions (Figure

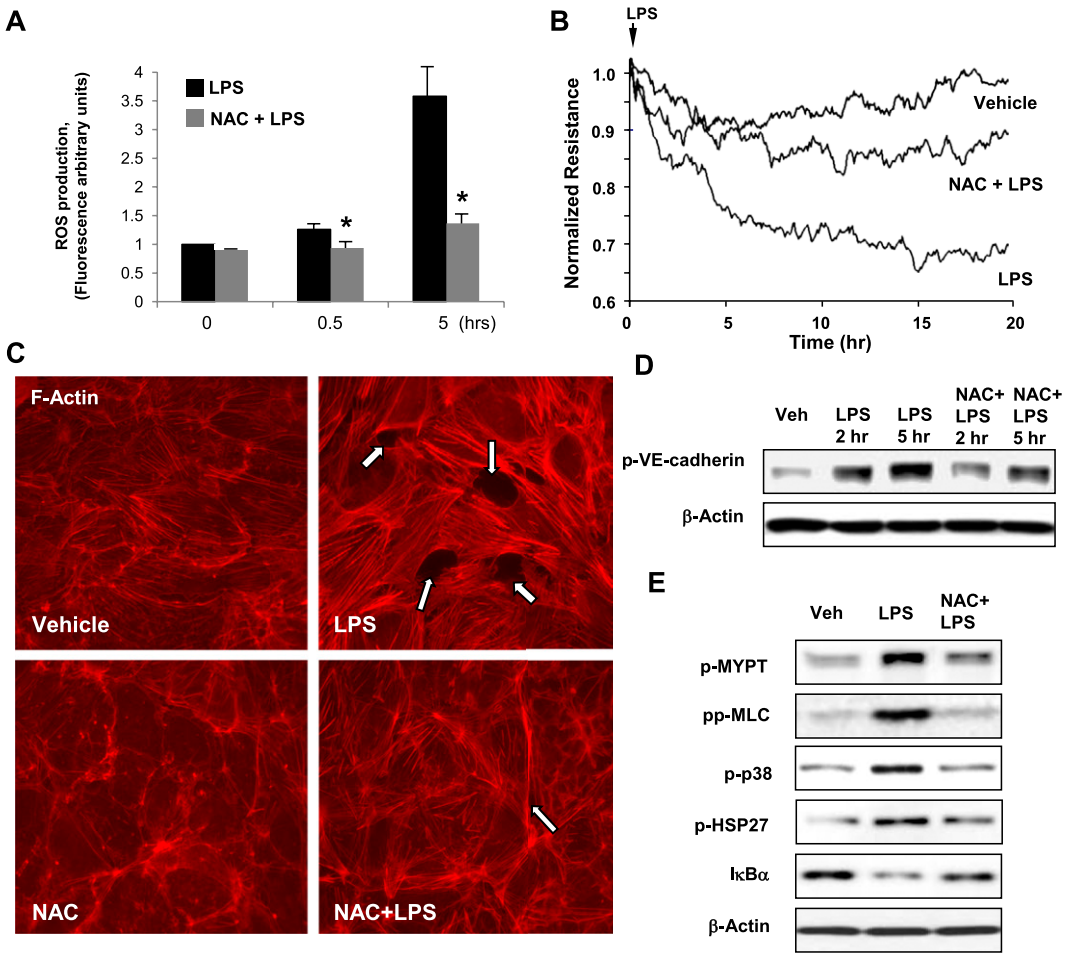

Figure 1. Role of oxidative stress in LPS-induced endothelial barrier disruption. Human pulmonary artery EC (HPAEC) monolayers were pretreated with vehicle or N-acetyl cysteine (NAC; 1×10^{-3} mol/L, 30 min) followed by LPS stimulation (300 ng/ml). (*A*) Reactive oxygen species (ROS) production was measured in live cells using fluorescent detection assay, as described in MATERIALS AND METHODS. Data are expressed as means (±SD) of three independent experiments; $*P < 0.05$. (*B*) Measurements of transendothelial electrical resistance (TER) were monitored over 20 hours using an electrical cell-substrate impedance sensing system. (*C*) Analysis of actin cytoskeletal rearrangement was performed after 5 hours of LPS treatment by immunofluorescence staining with Texas Red phalloidin. Paracellular gaps are marked by *arrows*. (*D* and *E*) Phosphorylation of VE-cadherin (*D*), myosin-associated phosphatase type 1 (MYPT1), myosin light chain (MLC), p38, and heat shock protein (HSP) 27 (*E*) was determined by Western blot with corresponding phospho-specific antibodies. Degradation of IκBα was detected using pan IκBα antibodies. Equal protein loading was confirmed by determination of β-actin content in total cell lysates. Results are representative of three to five independent experiments.

2D). Remarkably, suppression of oxidative stress by NAC restored levels of acetylated tubulin and decreased tubulin tyrosination in LPS-treated ECs (Figures 2C and 2D).

Direct induction of oxidative stress in pulmonary EC cultures by incubation with hydrogen peroxide demonstrated effects similar to LPS with regard to decreased polymerized tubulin content and reduced acetylated tubulin pool (Figure 2E). Taken together, our results strongly suggest the direct involvement of LPS-induced oxidative stress in the alteration of MT network.

MT Disassembly Mediates LPS-Induced Endothelial Permeability

The studies described subsequently here addressed involvement of the observed MT remodeling in the development of LPS-induced EC barrier dysfunction. In these experiments, LPS-induced MT disassembly was prevented by cell pretreatment with MT stabilizer, epothilone B. Control biochemical analysis of the MT-enriched fraction confirmed preservation of the pool of polymerized tubulin by epothilone B against LPS-induced depolymerization (Figure 3A). Next, we analyzed the effects of MT preservation by epothilone B on the LPS-induced EC barrier disruption. Cell pretreatment with epothilone B attenuated LPS-induced hyperpermeability (Figure 3B), stress fibers, and paracellular gap formation (Figure 3C), and suppressed LPS-induced activation of Rho, p38 MAPK, and NF-κB signaling (Figure 3D).

Role of MT-Associated GEF-H1 in the Mechanisms of LPS-Induced MT Disassembly

Because the activation state of Rho-specific GEF, GEF-H1, depends on its association with MTs, and Rho signaling in turn may additionally regulate MT dynamics (10, 29), we examined the involvement of GEF-H1 in the LPS-induced MT changes and EC barrier disruption. EC stimulation with LPS decreased GEF-H1 content in the MT fractions. Importantly, ROS blocking by NAC or MT stabilization by epothilone B prevented LPS-induced decrease in the GEF-H1 content observed in the MT fractions (Figures 4A and 4B).

Molecular inhibition of GEF-H1 using siRNA-based knockdown preserved the MT network in the LPS-treated ECs, as compared with LPS-challenged cells transfected with nonspecific RNA (Figure 4C). GEF-H1 knockdown also preserved the pool of acetylated tubulin against LPS-induced deacetylation (Figure 4D). In addition, LPS induced phosphorylation of MT regulatory protein, Tau, at Rho kinase–dependent sites, S^{262} and S^{409}, which leads to Tau dissociation from MTs and MT destabilization (30–32). This phosphorylation was inhibited by GEF-H1 knockdown (Figure 4D). These results demonstrate a positive feedback mechanism of additional MT disassembly by GEF-H1–

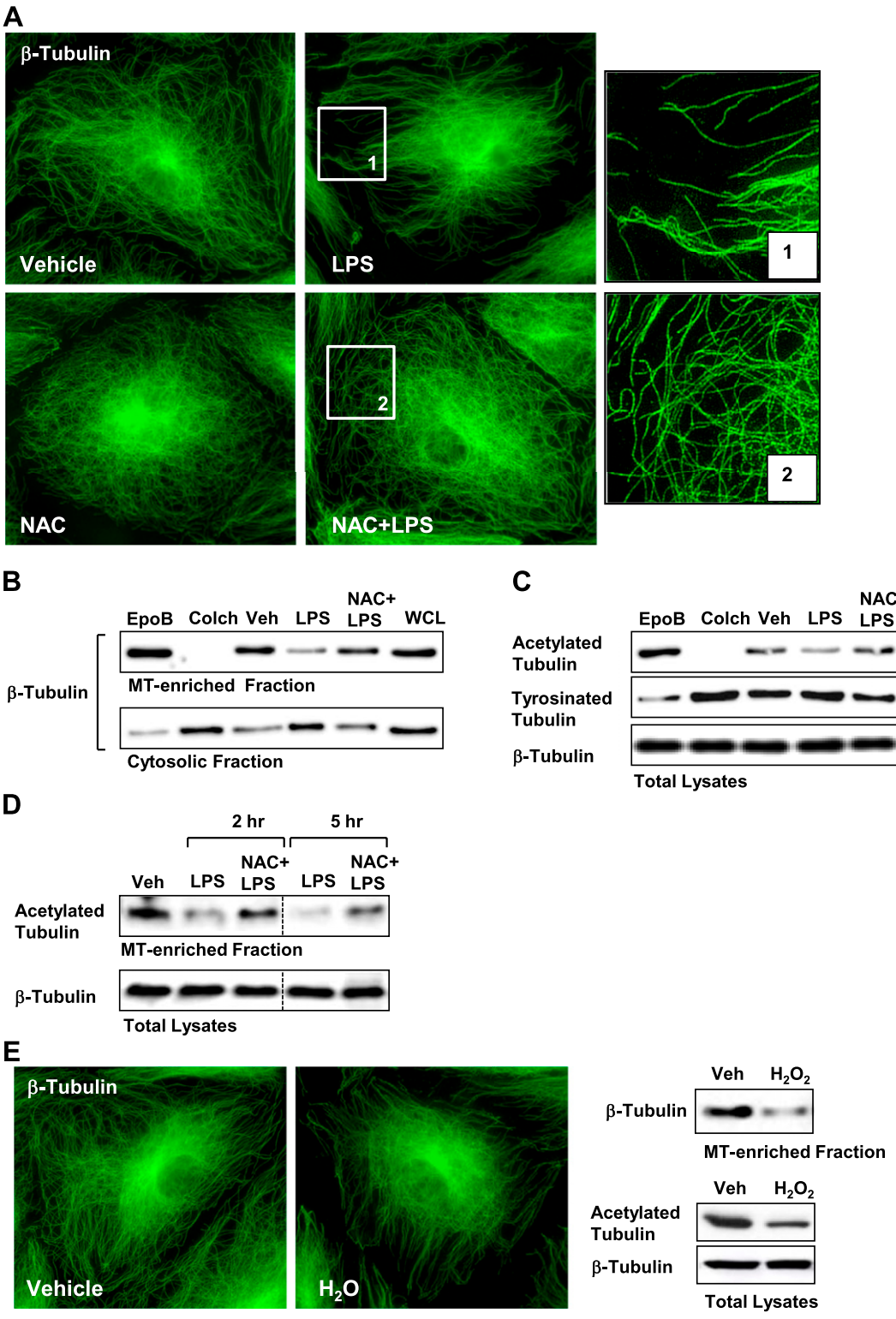

Figure 2. Role of oxidative stress in LPS-induced microtubule (MT) remodeling. Human pulmonary artery endothelial cells (HPAECs) were pretreated with vehicle or NAC (1×10^{-3} mol/L, 30 min) followed by LPS (300 ng/ml). In control experiments, cells were treated with epothilone B (EpoB; 1×10^{-8} mol/L) or colchicine (Colch; 1×10^{-6} mol/L) for 30 minutes. (*A*) MT structure was analyzed by immunofluorescence staining for β-tubulin. *Insets* indicate high-magnification images of peripheral MT network. (*B*) Fractionation assay was performed and content of polymerized tubulin in MT-enriched fraction and depolymerized tubulin in cytosolic fraction was determined by Western blotting with β-tubulin antibodies. (*C*) Pools of acetylated MTs and tyrosinated MTs were determined in whole-cell lysates. Equal tubulin content was confirmed by probing of membranes for β-tubulin. (*D*) Effects of NAC on LPS-induced alteration of stable MTs were evaluated by Western blot analysis of MT-enriched fraction with antibodies against acetylated tubulin. Equal tubulin expression was confirmed by detection of β-tubulin in total cell lysates. (*E*) Effect of H_2O_2 (1×10^{-4} mol/L, 15 min) on MT structure was analyzed by immunofluorescence staining (*upper panel*), determination of polymerized tubulin content in MT-enriched fraction (*lower left panel*), and detection of acetylated tubulin in total cell lysates (*lower right panel*). Results are representative of three to six independent experiments.

dependent Rho activation, which can be inhibited by GEF-H1 suppression.

Effects of GEF-H1 inhibition were further tested in the model of LPS-induced EC permeability. In comparison to LPS-stimulated EC monolayers transfected with nonspecific siRNA, GEF-H1 knockdown abolished the LPS-induced TER decrease, suggesting preservation of EC barrier function (Figure 5A). Down-regulation of GEF-H1 expression also attenuated cytoskeletal remodeling and intracellular signaling in response to LPS, characterized by a reduced number of paracellular gaps (Figure 5B), decreased VE-cadherin phosphorylation leading to preservation of cell–cell junctions, and inhibition of LPS-induced Rho, p38 MAPK, and NF-κB cascades (Figure 5C).

Role of MTs in LPS-Induced Inflammatory Endothelial Activation

Endothelial activation by inflammatory agonists plays an important role in the development of acute lung injury (ALI), because

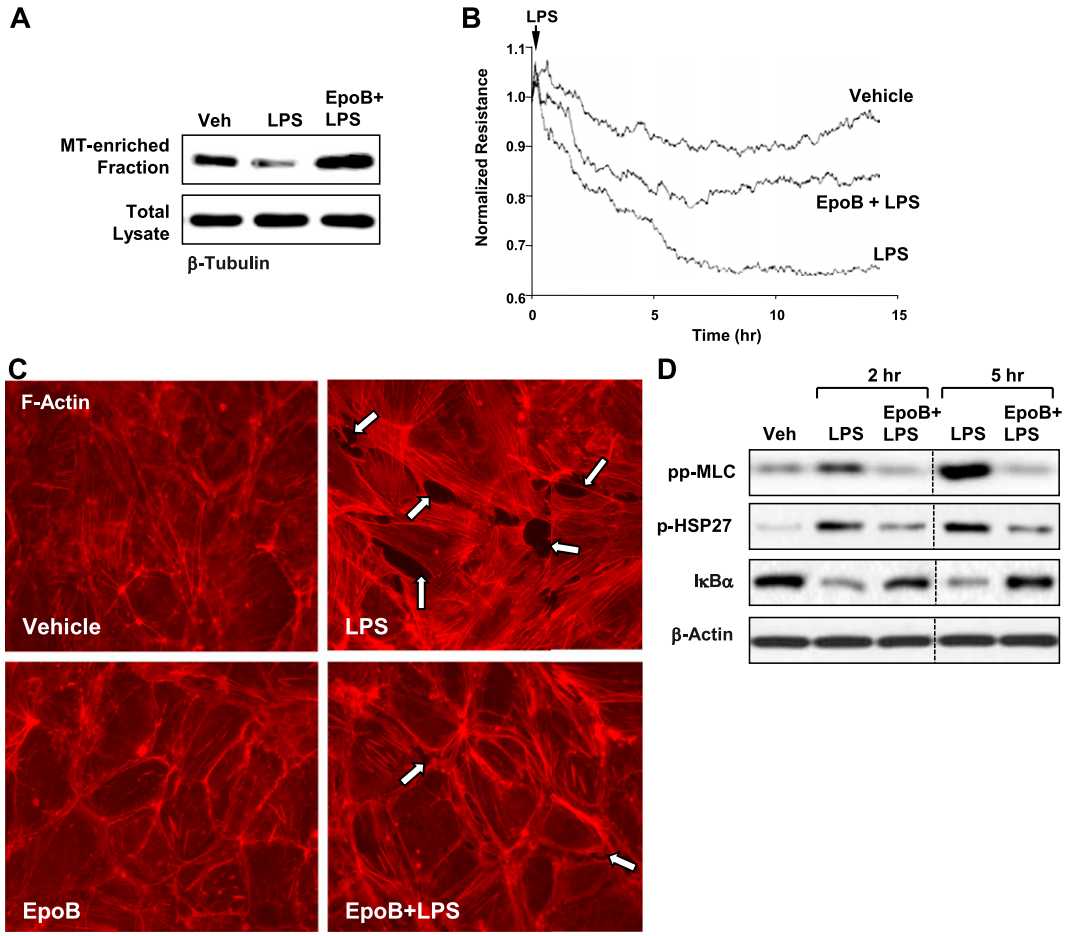

Figure 3. Effect of MT stabilization on LPS-induced EC barrier dysfunction. HPAECs were pretreated with vehicle or epothilone B (1×10^{-8} mol/L, 30 min) followed by LPS (300 ng/ml) stimulation. (*A*) Content of polymerized tubulin in MT-enriched fraction was determined by Western blot analysis with β-tubulin antibodies. Equal tubulin expression was confirmed by detection of β-tubulin in total cell lysates. (*B*) TER measurements were performed over 15 hours. (*C*) Actin cytoskeletal remodeling after 5 hours of LPS treatment was examined by immunofluorescence staining with Texas Red–conjugated phalloidin. Paracellular gaps are marked by *arrows*. (*D*) Phosphorylation of MLC and HSP27, or IκBα content was analyzed by Western blotting. Equal protein loading was confirmed by determination of β-actin content in total cell lysates. Shown are representative results of three to five independent experiments.

it stimulates neutrophil adhesion to the vascular ECs, followed by neutrophil transmigration through EC monolayer, and neutrophil infiltration to the lung parenchyma. We evaluated a role of MTs in LPS-induced endothelial activation. ICAM-1 is an endothelial surface adhesion molecule involved in neutrophil adhesion to the activated endothelium. LPS increased expression of ICAM-1 in the HPAECs, and this effect was significantly attenuated by EC pretreatment with NAC, MT stabilization by epothilone B, or siRNA-based GEF-H1 knockdown (Figures 6A and 6B).

Because LPS-induced production of proinflammatory cytokines by vascular endothelium is important for neutrophil transmigration as a second step of LPS-induced polymorphonuclear leukocytes (PMN) infiltration in the lung, we examined the role of MT stabilization and ROS inhibition on LPS-induced IL-8 production. LPS markedly increased IL-8 production by pulmonary ECs, which was significantly attenuated by pretreatment with epothilone B or NAC (Figure 6C). Next, we evaluated effects of preconditioned medium collected from LPS-stimulated EC cultures on directed neutrophil migration. LPS stimulation of EC cultures significantly increased neutrophil migration response to preconditioned medium from LPS-stimulated ECs, whereas EC pretreatment with epothilone B or NAC during LPS challenge suppressed neutrophil migration response (Figure 6D). Control PMN migration experiments using the same LPS dose added to fresh, nonpreconditioned culture medium showed background PMN migration rates compared with vehicle control (data not shown). Collectively, these data suggest potent protective effects of MT stabilization against activation of inflammatory signaling in pulmonary endothelium induced by LPS.

Role of MTs in the Development of LPS-Induced Lung Injury *In Vivo*

The role of MT-associated signaling was further tested in the septic model of ALI induced by intratracheal instillation of LPS. C57BL6 mice were challenged with LPS for 18 hours with or without epothilone B treatment, and lung injury was assessed by analysis of protein content and cell count in BAL fluid. Intratracheal LPS instillation caused pronounced increase in BAL protein concentration, total cell counts, and neutrophil counts (Figure 7A). Intravenous injection of epothilone B significantly decreased BAL protein content and reduced total and neutrophil cell counts in LPS-treated mice. In keeping with cell culture studies, MT stabilization also inhibited LPS-induced IκBα degradation and ICAM1 expression (Figure 7B), which was detected by Western blot analysis of lung tissue homogenates. We also evaluated the levels of acetylated tubulin, which represents a pool of stable MTs, in the lungs of mice exposed to LPS with and without NAC cotreatment. NAC markedly attenuated LPS-induced decrease in the acetylated tubulin content in the lung extracts (Figure 7C).

In the next studies, we performed *in vivo* knockdown of GEF-H1 using an siRNA approach. Mice were transfected with nonspecific or GEF-H1–specific siRNA for 72 hours, followed by LPS instillation for 18 hours. Similar to nontransfected animals (Figure 7A), in mice transfected with nonspecific RNA, LPS caused a prominent increase in BAL and protein concentration and total cell and neutrophil counts (Figure 7D), whereas GEF-H1 knockdown abolished these effects. Analysis of lung tissue samples also revealed a protective effect of GEF-H1 down-regulation against LPS-induced IκBα degradation and ICAM1 expression (Figure 7E). These results demonstrate the critical role of

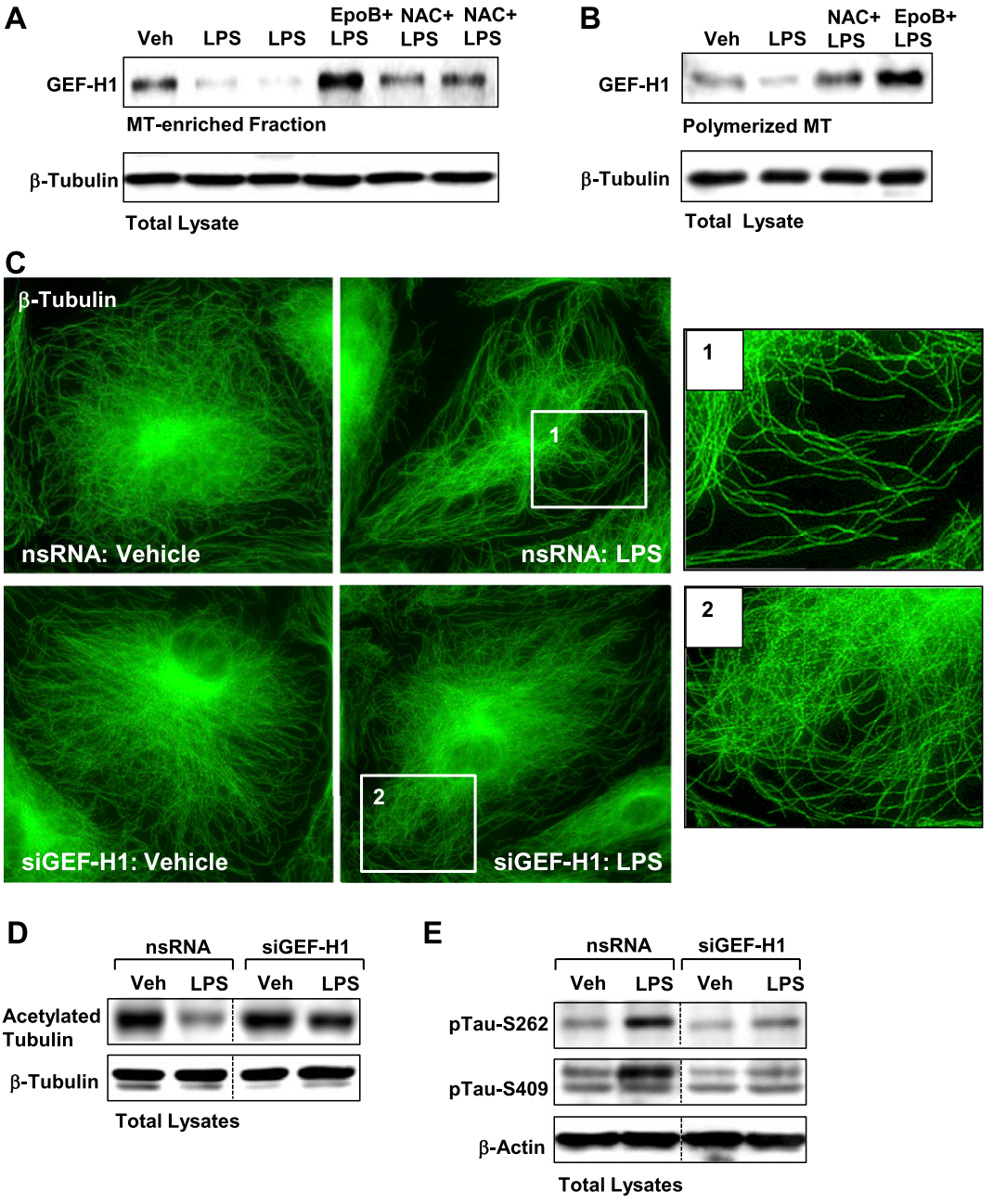

Figure 4. Role of MT-associated guanine nucleotide exchange factor (GEF)-H1 in LPS-induced MT alteration. ECs were pretreated with vehicle, NAC (1×10^{-3} mol/L, 30 min), or epothilone B (1×10^{-8} mol/L, 30 min), followed by LPS (300 ng/ml) stimulation for 5 hours. (*A* and *B*) GEF-H1 content in MT-enriched fraction (*A*) or polymerized MT fraction (*B*) was determined by Western blot analysis with specific antibodies. Equal tubulin content was confirmed by detection of β-tubulin in total cell lysates. (*C–E*) Human pulmonary ECs were transfected with GEF-H1–specific siRNA or nonspecific RNA followed by LPS stimulation. MT structure was analyzed by immunofluorescence staining for β-tubulin. *Insets* represent high-magnification images of peripheral MT network (*C*). Pool of stable MTs was determined by Western blot analysis with antibodies against acetylated tubulin. Equal tubulin content was confirmed by probing of membranes with β-tubulin antibodies (*D*). Tau phosphorylation after LPS challenge was analyzed by Western blot with specific antibodies. Equal protein loading was confirmed by determination of β-actin content in total cell lysates. Shown are representative results of three to four independent experiments.

MT-associated GEF-H1–dependent signaling in the development of septic inflammation and vascular endothelial barrier dysfunction in cell culture and animal models of LPS-induced lung injury.

DISCUSSION

A role of redox signaling in the activation of inflammatory pathways in the lungs upon LPS challenge is well recognized (33–35). The canonical pathway of NF-κB cascade activation by LPS involves activation of Toll-like receptor-4, leading to recruitment of the adaptor molecules, MyD88, IL-1R–associated kinase, and TNF receptor–associated factor 6, and activation of MAPKs, Jun amino-terminal kinase, p38, and extracellular signal–regulated kinase 1/2 (ERK 1/2) and IκB kinase complex, a cytoplasmic inhibitor of NF-κB (reviewed in Ref. 36). These cascades activate expression of inflammatory cytokines and surface adhesion molecules, leading to neutrophil and monocyte adhesion to vascular endothelium, extravasation, and activation of tissue inflammation.

In addition to this canonical pathway, LPS activates ROS production (7, 37, 38) and Rho signaling (39–42), and these mechanisms further enhance LPS-induced NF-κB and stress kinase activation. A recent report by Zhang and colleagues (43) shows Rho activation downstream of ROS production; however, the exact mechanism of this signaling sequence remained unclear. This study demonstrates, for the first time, the mechanism of activation of Rho signaling by LPS, which involves ROS-dependent MT destabilization and release of MT-associated GEF-H1. These events stimulate Rho-dependent EC permeability and activation of NF-κB cascade and p38 stress MAPK signaling.

LPS-induced MT disassembly was documented by immunofluorescence microscopy and additionally verified by a decreased pool of polymerized tubulin detected in a sedimentation assay. LPS also decreased the pool of stable MTs, as judged by decreased content of acetylated tubulin (26), and increased the pool of unstable (tyrosinylated) MTs (44). Both the ROS quencher, NAC, and MT stabilizer, epothilone B, prevented the LPS-induced

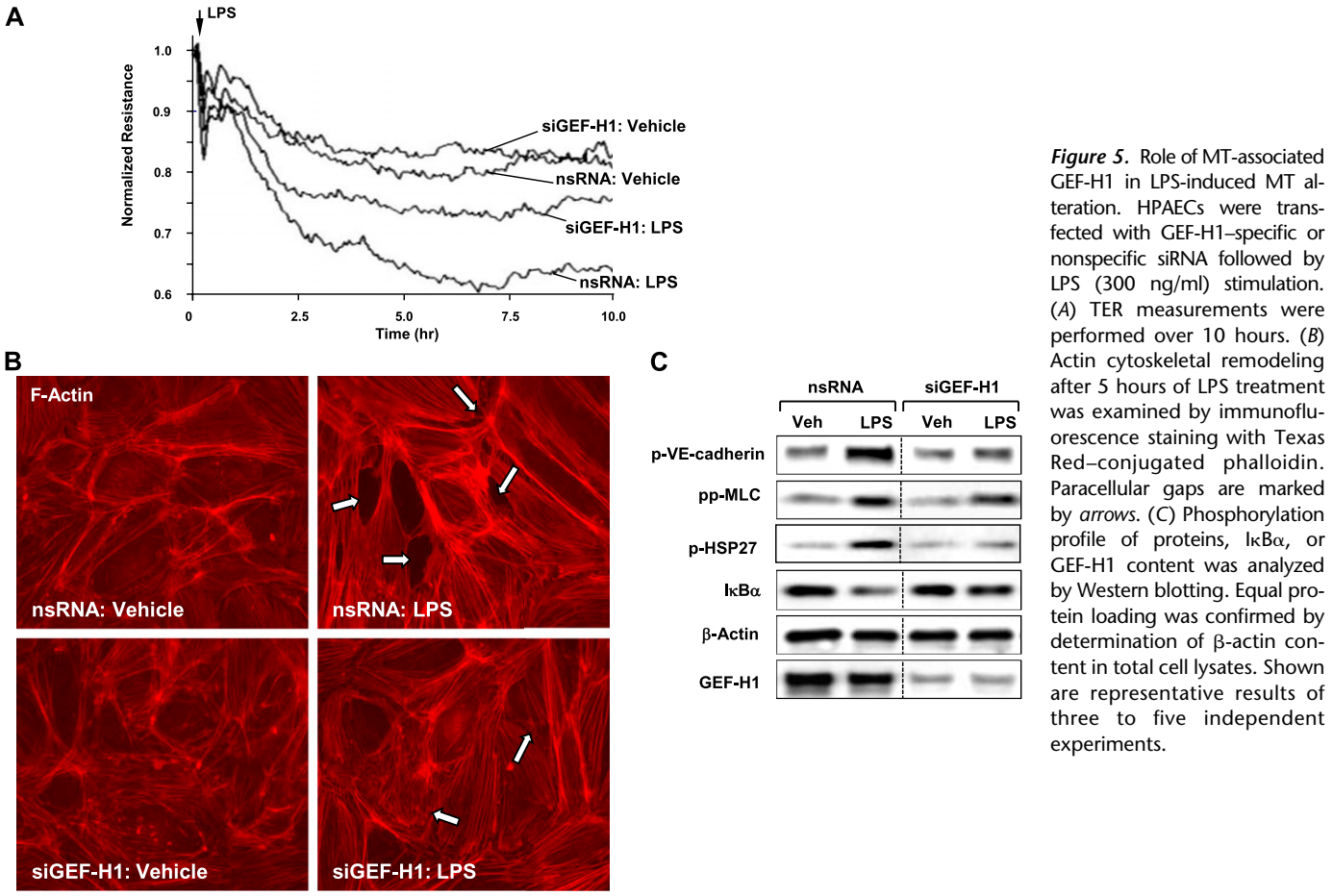

Figure 5. Role of MT-associated GEF-H1 in LPS-induced MT alteration. HPAECs were transfected with GEF-H1–specific or nonspecific siRNA followed by LPS (300 ng/ml) stimulation. (*A*) TER measurements were performed over 10 hours. (*B*) Actin cytoskeletal remodeling after 5 hours of LPS treatment was examined by immunofluorescence staining with Texas Red–conjugated phalloidin. Paracellular gaps are marked by *arrows*. (*C*) Phosphorylation profile of proteins, IκBα, or GEF-H1 content was analyzed by Western blotting. Equal protein loading was confirmed by determination of β-actin content in total cell lysates. Shown are representative results of three to five independent experiments.

MT disassembly and attenuated LPS-induced EC permeability. Collectively, these results suggest the direct link between redox-dependent control of the pool of polymerized MTs, Rho signaling, activation of NF-κB, and p38 stress kinase and EC barrier properties. In LPS-stimulated ECs, the MT-stabilizing effect of NAC was comparable to epothilone B. These data suggest that intrinsic redox signaling may serve as a critical regulator of MT dynamics and MT-dependent cellular processes. These interesting aspects of ROS-dependent regulation of cell functions require further investigation.

MT-associated Rho activator, GEF-H1, has been implicated in the activation of Rho signaling, contractile cell morphology, and EC permeability (10, 45, 46). Our results show LPS-induced release of GEF-H1 from MTs, which leads to its activation (29). GEF-H1 release from MT cytoskeleton was attenuated by NAC and epothilone B, and correlated with attenuation of LPS-induced EC permeability, p38 and NF-κB activation, ICAM-1 and IL-8 expression, and neutrophil adhesion to activated ECs. These results strongly support the mechanism of MT-dependent control of Rho signaling, EC permeability, and innate immunity response to LPS. It has been noted before that NF-κB, ERK 1/2, and p38/MK-2 MAPK pathways may be directly regulated in a redox-sensitive manner (37, 47, 48). The results of this study do not exclude this mechanism, but provide an additional MT-dependent mechanism of inflammatory signaling regulation by release and activation of MT-bound GEF-H1.

Knockdown of GEF-H1 using an siRNA approach attenuated LPS-induced EC permeability, stress fibers and paracellular gap formation in EC monolayers, decreased phosphorylation of MLC, VE-cadherin, p38 stress kinase target, HSP-27, and suppressed LPS-induced degradation of the NF-κB inhibitory subunit, IκBα. As a result, GEF-H1 knockdown suppressed LPS-induced activation of ICAM-1 and IL-8 expression and neutrophil adhesion. Interestingly, besides effects on EC permeability, GEF-H1 knockdown also partially suppressed LPS-induced MT disassembly and prevented a decline in the stable (acetylated) MT pool. These results suggest a positive feedback mechanism of MT control by GEF-H1. Tau is another MT-associated protein that stabilizes polymerized MTs, whereas tau phosphorylation by several kinases decreases its capacity to bind MTs and leads to MT disassembly (30, 31). Tau amino acid residues Ser^{262} and Ser^{409} have been identified as Rho kinase–mediated phosphorylation sites (32), and our previous studies demonstrated that Rho kinase–mediated tau phosphorylation decreased MT assembly (13, 14). Our results show LPS-induced tau phosphorylation at Ser^{262} and Ser^{409}, which was abolished by GEF-H1 knockdown. In agreement with the role of tau in the MT stabilization, inhibition of Rho kinase–mediated tau phosphorylation as a result of GEF-H1 knockdown also partially prevented MTs from LPS-induced disassembly. These data suggest the positive feedback activation of Rho signaling via the following mechanism: LPS-induced partial MT disassembly → dissociation and activation of GEF-H1 → stimulation of Rho-Rho kinase → phosphorylation of tau → further destabilization of MT cytoskeleton → additional GEF-H1 release and propagation of Rho signaling. It is also important to note that initiation, plateau, and resolution phases of inflammatory response are controlled by multiple and complex mechanisms. Subsiding inflammation leads to reduction of ROS production, which reverses ROS-induced MT instability, promotes the restoration of MT network structure, and increases the pool of MT-bound (inactivated) GEF-H1. Thus, restoration of native

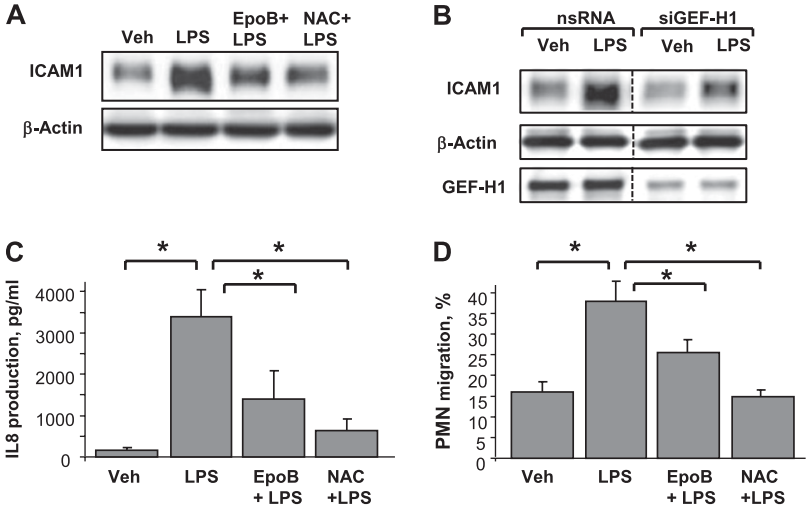

Figure 6. Role of MTs in LPS-induced endothelial activation. (*A*) ECs were pretreated with vehicle, NAC (1×10^{-3} mol/L, 30 min), or epothilone B (1×10^{-8} mol/L, 30 min) followed by LPS (300 ng/ml) stimulation for 5 hours. Intercellular adhesion molecule (ICAM)-1 expression was detected by Western blot with specific antibodies. β-actin staining was used as a normalization control. (*B*) HPAECs were transfected with GEF-H1–specific or nonspecific siRNA followed by LPS stimulation (300 ng/ml, 5 h). ICAM-1 expression was detected by Western blot analysis. Equal protein loading was confirmed by determination of β-actin content in total cell lysates. (*C* and *D*) Cells were pretreated with vehicle, NAC (1×10^{-3} mol/L, 30 min), or epothilone B (1×10^{-8} mol/L, 30 min) followed by LPS stimulation (20 ng/ml, 4 h). IL-8 production was determined in control and treated samples using an ELISA kit (*C*). Neutrophil migration assay was performed as described in MATERIALS AND METHODS (*D*). Data are expressed as means (±SD) of five independent experiments; $^*P < 0.05$.

MT structure under normalized redox conditions may be very rapid.

MT destabilization upon LPS treatment may also involve alternative mechanisms and be controlled by ROS-dependent tubulin oxidation. Tubulin oxidation demonstrated in cells treated with certain anticancer agents was associated with reduced tubulin polymerization (49, 50), although these additional mechanisms were not addressed in this study.

In addition to protective effects of MT stabilization and GEF-H1 knockdown against LPS-induced permeability and inflammatory activation in pulmonary EC cultures, attenuation of LPS-induced lung dysfunction and inflammation was also

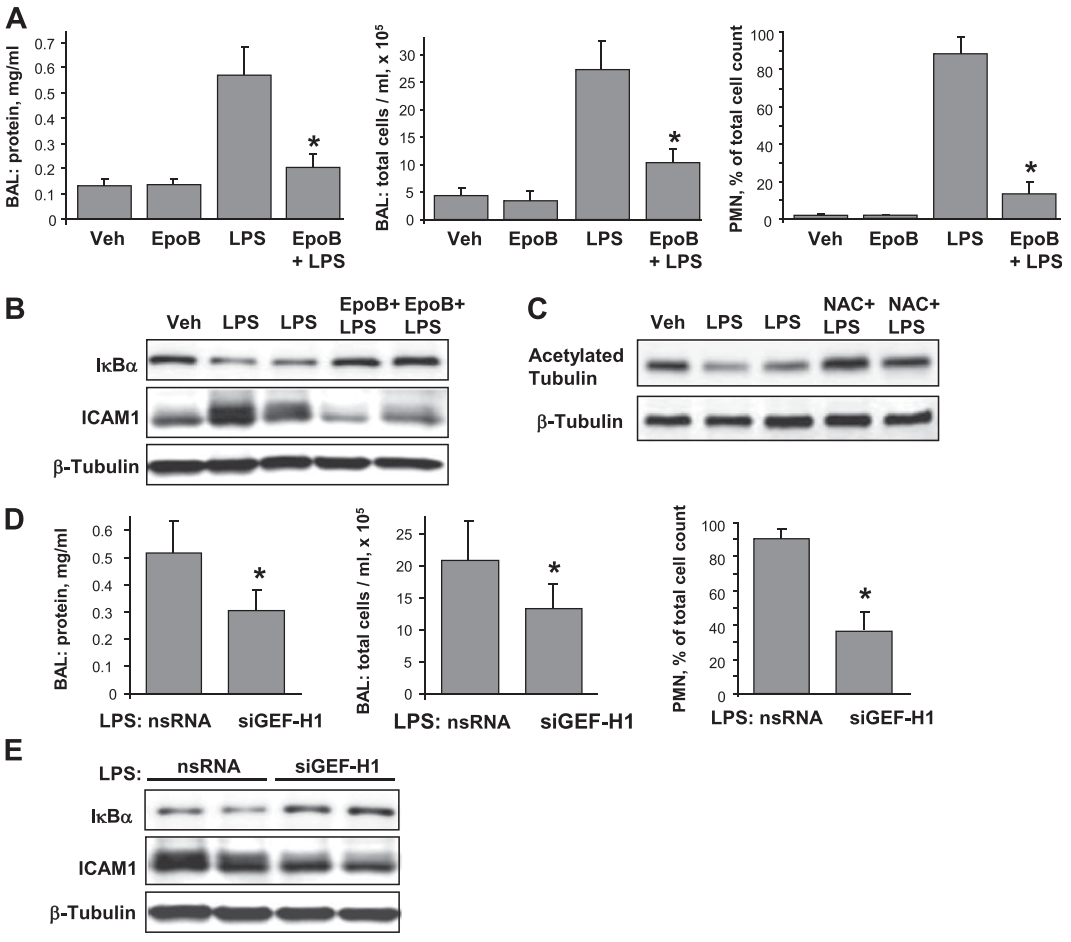

Figure 7. Role of MTs in LPS-induced lung injury. (*A–C*) C57BL/6J mice were challenged with LPS (0.63 mg/kg, intratracheally) with or without concurrent intravenous injection of epothilone B (4×10^{-6} mol/kg, intravenously) or NAC (2.5×10^{-3} mol/kg). Control animals were treated with sterile saline solution or epothilone B alone. (*A*) Protein concentration, total cell count, and neutrophil count were determined in bronchoalveolar lavage fluid collected 18 hours after treatments. Data are expressed as means (±SD) ($n = 4–8$ per condition); $^*P < 0.05$, as compared with LPS treatment. (*B*) IκBα degradation and ICAM1 expression after LPS challenge with or without epothilone B treatment were determined in lung tissue homogenates by Western blot analysis with specific antibodies. Equal protein loading was confirmed by membrane reprobing with β-tubulin antibodies. (*C*) Levels of acetylated tubulin after LPS challenge with or without NAC treatment were determined in lung tissue homogenates by Western blot analysis with specific antibodies. Equal protein loading was confirmed by membrane reprobing with β-tubulin antibodies. (*D* and *E*) Mice were transfected with nonspecific or GEF-H1–specific siRNA for 72 hours followed by LPS (0.63 mg/kg, intratracheally) administration for 18 hours. (*C*) protein concentration, total cell count, and neutrophil count were determined in bronchoalveolar lavage fluid. Data are expressed as means (±SD) ($n = 4–6$ per condition; $^*P < 0.05$). (*D*) IκBα degradation and ICAM1 expression after LPS challenge were determined in lung tissue homogenates from nonspecific or GEF-H1–specific siRNA-treated mice by Western blot analysis. Equal protein loading was confirmed by membrane reprobing with β-tubulin antibodies.

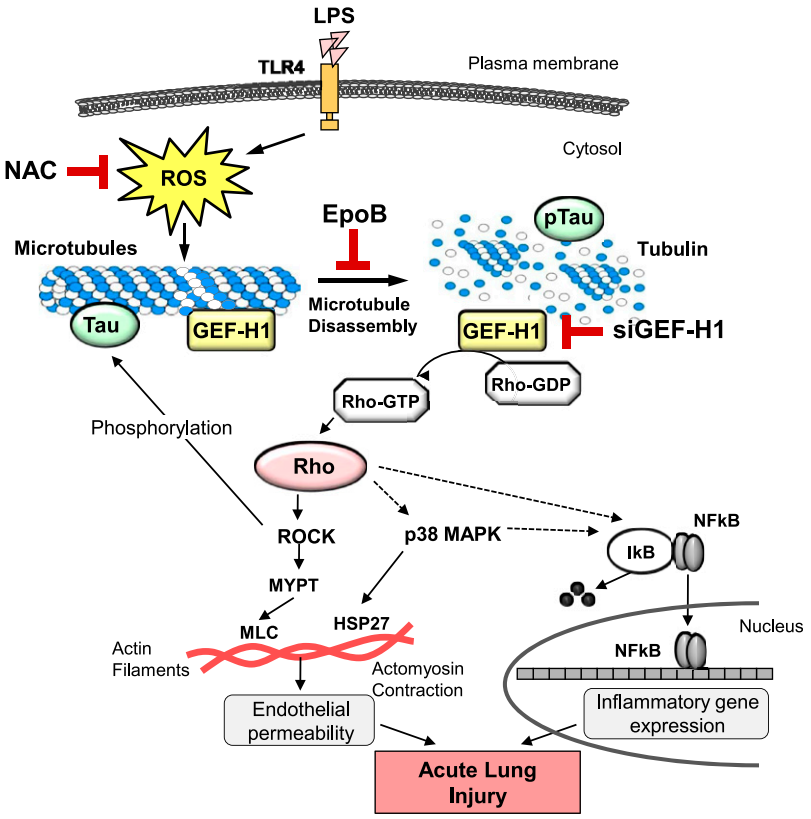

Figure 8. Proposed model of MT-dependent signaling in LPS-challenged lung endothelium (*see* explanation in the main text).

observed in mice with GEF-H1 knockdown or in LPS-challenged mice treated with epothilone B or NAC. In agreement with these data, treatment with another NAC-like antioxidant compound, amifostine, was also protective against LPS-induced lung vascular permeability and inflammation *in vivo* (21). Altogether, these data demonstrate that prevention of LPS-induced MT destabilization by antioxidants or direct stabilizers of MTs down-regulates GEF-H1–dependent Rho signaling and contributes to both increased vascular permeability and inflammatory effects of LPS.

Our results show direct involvement of GEF-H1 in the two pathologic Rho-dependent cascades triggered by LPS: lung vascular leak and inflammation. GEF-H1 inhibition has also been observed to be protective in the model of ventilator-induced lung injury (46). Besides functional activation, expression levels of GEF-H1 can be additionally stimulated by LPS (51), bringing about an even more significant role for GEF-H1 in LPS-induced lung dysfunction. Because these two conditions are often intertwined in clinical practice, and may lead to severe ALI/acute respiratory distress syndrome and high mortality, pharmacologic targeting of GEF-H1 may be strongly considered as a therapeutic option. Taken together, these data strongly support the novel mechanism of modulation of LPS-induced innate immune response and lung injury *in vivo* via redox-dependent regulation of MT stability and GEF-H1/Rho signaling.

In summary, this work describes a novel role of MTs in the regulation of EC responses triggered by inflammatory agonists. We have demonstrated, for the first time, the redox-sensitive mechanism of Rho pathway activation by MT-associated GEF-H1. Based on these results, we propose the following model of MT-dependent signaling in LPS-treated ECs (Figure 8): LPS treatment activates ROS production by ECs via activation of reduced nicotinamide adenine dinucleotide phosphate oxidase (6, 7) or xanthine oxidoreductase (8), which promotes partial MT disassembly by yet-to-be-defined mechanisms; one mechanism may involve direct tubulin oxidation. MT disassembly results in dissociation of GEF-H1 from MTs and its activation, which stimulates Rho signaling and Rho-dependent potentiation of stress kinases and NF-κB cascade, thus leading to EC barrier dysfunction, activation of IL-8 and ICAM-1 expression by pulmonary ECs, and IL-8–mediated PMN migration. The results of this study suggest that therapeutic strategies directed at mitigation of oxidative stress, stabilization of MTs, and suppression of GEF-H1 activities in the settings of ALI may be a promising direction for future drug design.

Author disclosures are available with the text of this article at www.atsjournals.org.

Acknowledgments: The authors thank Katherine Higginbotham for proofreading and editing the manuscript.

References

1. Mehta D, Malik AB. Signaling mechanisms regulating endothelial permeability. *Physiol Rev* 2006;86:279–367.
2. Lucas R, Verin AD, Black SM, Catravas JD. Regulators of endothelial and epithelial barrier integrity and function in acute lung injury. *Biochem Pharmacol* 2009;77:1763–1772.
3. Dosquet C, Weill D, Wautier JL. Molecular mechanism of blood monocyte adhesion to vascular endothelial cells. *Nouv Rev Fr Hematol* 1992; 34:S55–S59.
4. Wang Q, Doerschuk CM. The signaling pathways induced by neutrophil–endothelial cell adhesion. *Antioxid Redox Signal* 2002;4:39–47.
5. Smith CW. Leukocyte–endothelial cell interactions. *Semin Hematol* 1993;30(4 Suppl 4):45–53; discussion 54–45.
6. Chen W, Pendyala S, Natarajan V, Garcia JG, Jacobson JR. Endothelial cell barrier protection by simvastatin: GTPase regulation and NADPH oxidase inhibition. *Am J Physiol Lung Cell Mol Physiol* 2008;295:L575–L583.
7. Maitra U, Singh N, Gan L, Ringwood L, Li L. IRAK-1 contributes to lipopolysaccharide-induced reactive oxygen species generation in macrophages by inducing NOX-1 transcription and RAC1 activation and suppressing the expression of antioxidative enzymes. *J Biol Chem* 2009;284:35403–35411.
8. Hassoun PM, Yu FS, Cote CG, Zulueta JJ, Sawhney R, Skinner KA, Skinner HB, Parks DA, Lanzillo JJ. Upregulation of xanthine oxidase

by lipopolysaccharide, interleukin-1, and hypoxia: role in acute lung injury. *Am J Respir Crit Care Med* 1998;158:299–305.
9. Bulua AC, Simon A, Maddipati R, Pelletier M, Park H, Kim KY, Sack MN, Kastner DL, Siegel RM. Mitochondrial reactive oxygen species promote production of proinflammatory cytokines and are elevated in TNFR1-associated periodic syndrome (TRAPS). *J Exp Med* 2011;208:519–533.
10. Birukova AA, Adyshev D, Gorshkov B, Bokoch GM, Birukov KG, Verin AA. GEF-H1 is involved in agonist-induced human pulmonary endothelial barrier dysfunction. *Am J Physiol Lung Cell Mol Physiol* 2006;290:L540–L548.
11. Birukov KG, Bochkov VN, Birukova AA, Kawkitinarong K, Rios A, Leitner A, Verin AD, Bokoch GM, Leitinger N, Garcia JG. Epoxycyclopentenone-containing oxidized phospholipids restore endothelial barrier function via CDC42 and RAC. *Circ Res* 2004;95:892–901.
12. Birukova AA, Cokic I, Moldobaeva N, Birukov KG. Paxillin is involved in the differential regulation of endothelial barrier by HGF and VEGF. *Am J Respir Cell Mol Biol* 2008;40:99–107.
13. Birukova AA, Birukov KG, Smurova K, Adyshev DM, Kaibuchi K, Alieva I, Garcia JG, Verin AD. Novel role of microtubules in thrombin-induced endothelial barrier dysfunction. *FASEB J* 2004;18:1879–1890.
14. Tar K, Birukova AA, Csortos C, Bako E, Garcia JG, Verin AD. Phosphatase 2A is involved in endothelial cell microtubule remodeling and barrier regulation. *J Cell Biochem* 2004;92:534–546.
15. Solomon F. Direct identification of microtubule-associated proteins by selective extraction of cultured cells. *Methods Enzymol* 1986;134:139–147.
16. Yu JZ, Dave RH, Allen JA, Sarma T, Rasenick MM. Cytosolic g{alpha}s acts as an intracellular messenger to increase microtubule dynamics and promote neurite outgrowth. *J Biol Chem* 2009;284:10462–10472.
17. Birukova AA, Chatchavalvanich S, Rios A, Kawkitinarong K, Garcia JG, Birukov KG. Differential regulation of pulmonary endothelial monolayer integrity by varying degrees of cyclic stretch. *Am J Pathol* 2006;168:1749–1761.
18. Meliton AY, Munoz NM, Meliton LN, Binder DC, Osan CM, Zhu X, Dudek SM, Leff AR. Cytosolic group IVA phospholipase A2 mediates IL-8/CXCL8–induced transmigration of human polymorphonuclear leukocytes *in vitro*. *J Inflamm (Lond)* 2010;7:14.
19. Birukova AA, Malyukova I, Mikaelyan A, Fu P, Birukov KG. TIAM1 and betaPIX mediate RAC-dependent endothelial barrier protective response to oxidized phospholipids. *J Cell Physiol* 2007;211:608–617.
20. Birukova AA, Fu P, Chatchavalvanich S, Burdette D, Oskolkova O, Bochkov VN, Birukov KG. Polar head groups are important for barrier protective effects of oxidized phospholipids on pulmonary endothelium. *Am J Physiol Lung Cell Mol Physiol* 2007;292:L924–L935.
21. Fu P, Birukova AA, Xing J, Sammani S, Murley JS, Garcia JG, Grdina DJ, Birukov KG. Amifostine reduces lung vascular permeability via suppression of inflammatory signalling. *Eur Respir J* 2009;33:612–624.
22. Potter MD, Barbero S, Cheresh DA. Tyrosine phosphorylation of VE-cadherin prevents binding of p120- and beta-catenin and maintains the cellular mesenchymal state. *J Biol Chem* 2005;280:31906–31912.
23. Dejana E, Orsenigo F, Lampugnani MG. The role of adherens junctions and VE-cadherin in the control of vascular permeability. *J Cell Sci* 2008;121:2115–2122.
24. Birkenfeld J, Nalbant P, Yoon SH, Bokoch GM. Cellular functions of GEF-H1, a microtubule-regulated Rho-GEF: is altered GEF-H1 activity a crucial determinant of disease pathogenesis? *Trends Cell Biol.* 2008;18:210–219.
25. Nogales E. Structural insights into microtubule function. *Annu Rev Biochem* 2000;69:277–302.
26. Piperno G, LeDizet M, Chang XJ. Microtubules containing acetylated alpha-tubulin in mammalian cells in culture. *J Cell Biol* 1987;104:289–302.
27. Palazzo AF, Eng CH, Schlaepfer DD, Marcantonio EE, Gundersen GG. Localized stabilization of microtubules by integrin- and FAK-facilitated Rho signaling. *Science* 2004;303:836–839.
28. Palazzo AF, Cook TA, Alberts AS, Gundersen GG. Mdia mediates Rho-regulated formation and orientation of stable microtubules. *Nat Cell Biol* 2001;3:723–729.
29. Krendel M, Zenke FT, Bokoch GM. Nucleotide exchange factor GEF-H1 mediates cross-talk between microtubules and the actin cytoskeleton. *Nat Cell Biol* 2002;4:294–301.
30. Singh TJ, Grundke-Iqbal I, McDonald B, Iqbal K. Comparison of the phosphorylation of microtubule-associated protein tau by non-proline dependent protein kinases. *Mol Cell Biochem* 1994;131:181–189.
31. Gupta RP, Abou-Donia MB. Tau phosphorylation by diisopropyl phosphorofluoridate (DFP)–treated hen brain supernatant inhibits its binding with microtubules: role of Ca^{2+}/calmodulin–dependent protein kinase II in tau phosphorylation. *Arch Biochem Biophys* 1999;365:268–278.
32. Amano M, Kaneko T, Maeda A, Nakayama M, Ito M, Yamauchi T, Goto H, Fukata Y, Oshiro N, Shinohara A, *et al*. Identification of tau and MAP2 as novel substrates of Rho-kinase and myosin phosphatase. *J Neurochem* 2003;87:780–790.
33. Sprong RC, Winkelhuyzen-Janssen AM, Aarsman CJ, van Oirschot JF, van der Bruggen T, van Asbeck BS. Low-dose N-acetylcysteine protects rats against endotoxin-mediated oxidative stress, but high-dose increases mortality. *Am J Respir Crit Care Med* 1998;157:1283–1293.
34. Bhatia M, Moochhala S. Role of inflammatory mediators in the pathophysiology of acute respiratory distress syndrome. *J Pathol* 2004;202:145–156.
35. Tasaka S, Amaya F, Hashimoto S, Ishizaka A. Roles of oxidants and redox signaling in the pathogenesis of acute respiratory distress syndrome. *Antioxid Redox Signal* 2008;10:739–753.
36. Lu YC, Yeh WC, Ohashi PS. LPS/TLR4 signal transduction pathway. *Cytokine* 2008;42:145–151.
37. Haddad JJ, Land SC. Redox/ROS regulation of lipopolysaccharide-induced mitogen-activated protein kinase (MAPK) activation and MAPK-mediated TNF-alpha biosynthesis. *Br J Pharmacol* 2002;135:520–536.
38. Sanlioglu S, Williams CM, Samavati L, Butler NS, Wang G, McCray PB Jr, Ritchie TC, Hunninghake GW, Zandi E, Engelhardt JF. Lipopolysaccharide induces RAC1-dependent reactive oxygen species formation and coordinates tumor necrosis factor-alpha secretion through IKK regulation of NF-kappa B. *J Biol Chem* 2001;276:30188–30198.
39. Essler M, Staddon JM, Weber PC, Aepfelbacher M. Cyclic AMP blocks bacterial lipopolysaccharide-induced myosin light chain phosphorylation in endothelial cells through inhibition of Rho/Rho kinase signaling. *J Immunol* 2000;164:6543–6549.
40. Tasaka S, Koh H, Yamada W, Shimizu M, Ogawa Y, Hasegawa N, Yamaguchi K, Ishii Y, Richer SE, Doerschuk CM, *et al*. Attenuation of endotoxin-induced acute lung injury by the Rho-associated kinase inhibitor, Y-27632. *Am J Respir Cell Mol Biol* 2005;32:504–510.
41. Xing J, Birukova AA. Anp attenuates inflammatory signaling and rho pathway of lung endothelial permeability induced by LPS and TNFalpha. *Microvasc Res* 2010;79:26–62.
42. Xiaolu D, Jing P, Fang H, Lifen Y, Liwen W, Ciliu Z, Fei Y. Role of p115RhoGEF in lipopolysaccharide-induced mouse brain microvascular endothelial barrier dysfunction. *Brain Res* 2011;1387:1–7.
43. Zhang Y, Peng F, Gao B, Ingram AJ, Krepinsky JC. Mechanical strain–induced RhoA activation requires NADPH oxidase–mediated ROS generation in caveolae. *Antioxid Redox Signal* 2010;13:959–973.
44. Schulze E, Asai DJ, Bulinski JC, Kirschner M. Posttranslational modification and microtubule stability. *J Cell Biol* 1987;105:2167–2177.
45. Chang YC, Nalbant P, Birkenfeld J, Chang ZF, Bokoch GM. GEF-H1 couples nocodazole-induced microtubule disassembly to cell contractility via RhoA. *Mol Biol Cell* 2008;19:2147–2153.
46. Birukova AA, Fu P, Xing J, Yakubov B, Cokic I, Birukov KG. Mechanotransduction by GEF-H1 as a novel mechanism of ventilator-induced vascular endothelial permeability. *Am J Physiol Lung Cell Mol Physiol* 2010;298:L837–L848.
47. Lee K, Esselman WJ. Inhibition of ptps by H(2)O(2) regulates the activation of distinct MAPK pathways. *Free Radic Biol Med* 2002;33:1121–1132.
48. Haddad JJ, Olver RE, Land SC. Antioxidant/pro-oxidant equilibrium regulates HIF-1alpha and NF-kappa B redox sensitivity: evidence for inhibition by glutathione oxidation in alveolar epithelial cells. *J Biol Chem* 2000;275:21130–21139.
49. Huber K, Patel P, Zhang L, Evans H, Westwell AD, Fischer PM, Chan S, Martin S. 2-[(1-methylpropyl)dithio]-1H-imidazole inhibits tubulin polymerization through cysteine oxidation. *Mol Cancer Ther* 2008;7:143–151.
50. Kim SY, An JM, Lee HG, Du SK, Cheong CU, Seo JT. 1H-[1,2,4]oxadiazolo[4,3-a]quinoxalin-1-one induces cell cycle arrest and apoptosis in HeLa cells by preventing microtubule polymerization. *Biochem Biophys Res Commun* 2011;408:287–292.
51. Guo F, Xing Y, Zhou Z, Dou Y, Tang J, Gao C, Huan J. Guanine-nucleotide exchange factor-H1 mediates lipopolysaccharide-induced interleukin-6 and tumor necrosis factor alpha expression in endothelial cells via activation of nuclear factor-kappa-B. *Shock* 2012;37:531–538.